Life Sciences 207 (2018) 395–411

Contents lists available at ScienceDirect

Life Sciences

journal homepage: www.elsevier.com/locate/lifescie

Human melanoma-derived ectosomes are enriched with specific glycan epitopes☆

Magdalena Surman[a], Dorota Hoja-Łukowicz[a], Sabina Szwed[a], Anna Drożdż[b], Ewa Stępień[b], Małgorzata Przybyło[a,*]

[a] Department of Glycoconjugate Biochemistry, Institute of Zoology and Biomedical Research, Jagiellonian University in Kraków, ul. Gronostajowa 9, Kraków, Poland
[b] Department of Medical Physics, M. Smoluchowski Institute of Physics, Jagiellonian University in Kraków, ul. Łojasiewicza 11, Kraków, Poland

ARTICLE INFO

Keywords:
Extracellular vesicles
Glycosylation
Lectins
Melanoma
N-glycans

ABSTRACT

Aims: Numerous studies confirmed the involvement of extracellular vesicles in cancer development and progression. The present study was designed to investigate the glycan composition of ectosomes derived by human cutaneous melanoma (CM) cell lines with the use of lectins.

Main methods: Ectosomes released by primary (WM115, WM793) and metastatic (WM266-4, WM1205Lu) CM cells were isolated from conditioned media by sequential centrifugation. Proteins from ectosomes, the whole cell extracts and membrane fractions were probed with a panel of lectins using Western Blot and flow cytometry and compared in terms of disease stage and glycosignature.

Key findings: Ectosomal proteins revealed enrichment (mainly with fucose and complex type *N*-glycans with bisecting GlcNAc) or depletion of specific glycoepitopes in comparison to the parental cell membranes. Moreover, similar lectin binding patterns were observed between related cell lines. It is the first study to characterize the glycosylation of ectosome proteins released by CM cells.

Significance: Our data indirectly supports the findings that ectosomes derive from particular regions of the cell membrane contain a unique glycan composition, which could serve as a specific sorting signal. If proven correct, the hypothesis that glycan-based protein sorting is a major mechanism for protein incorporation into ectosomes may provide new means to control vesicular content and have possible clinical implications.

1. Introduction

Cancer development and progression are mainly dependent upon significant changes in the tumor microenvironment which has the impact on intercellular communication. Bioactive molecules involved in carcinogenesis, such as signaling factors, structural proteins, nucleic acids or lipids, can be delivered to target cells *via* extracellular vesicles (EVs) [1, 2]. EVs are small, membrane-enclosed particles, released by almost all cell types to the intercellular space. Based on their size, density, biogenesis and marker proteins, EVs are classified into three distinct populations - exosomes, ectosomes and apoptotic bodies. Ectosomes represent a fairly heterogeneous population of vesicles with a diameter ranging from 0.1 to 1 μm. The specific content of ectosomes and their action towards recipient cells depend on their molecular composition which is determined by the cell of their origin. Under physiological and pathological conditions, ectosomes are involved in the control and modulation of multiple biological processes, including coagulation, local inflammation, cell proliferation and differentiation, vascular senescence and tissue remodeling [3].

Increased amounts of EVs are associated with different disease states, including tumors. Tumor-derived EVs (TEVs) directly promote invasion, metastasis and angiogenesis or influence the changes in the tumor microenvironment [4–6]. TEVs may also facilitate cellular efflux of commonly used chemotherapeutics, thereby contributing to multidrug resistance. Fusion of TEVs with immune cells often leads to the alteration or inhibition of the immune response towards cancer cells. Thus, TEVs appear as a promising goal to identify novel cancer biomarkers.

☆ Authors' contributions: MP and DHŁ conceived the idea and planned the research. MP supervised the project. MS, MP, DHŁ and SS carried out the cell culture, ectosome isolation and lectin blotting. MS, MP and AD carried out the flow cytometry analysis. MS, MP, AD and ES performed data analysis. MS wrote the manuscript and prepared the figures. All authors discussed the results, aided in their interpreting, commented on the manuscript, contributed to its final version. All authors have approved the final article.

* Corresponding author at: Department of Glycoconjugate Biochemistry, Institute of Zoology and Biomedical Research, Jagiellonian University in Kraków, ul. Gronostajowa 9, 30-387 Kraków, Poland.

E-mail addresses: magdalena.surman@doctoral.uj.edu.pl (M. Surman), dorota.hoja-lukowicz@uj.edu.pl (D. Hoja-Łukowicz), sabina.szwed@doctoral.uj.edu.pl (S. Szwed), anna.drozdz@uj.edu.pl (A. Drożdż), e.stepien@uj.edu.pl (E. Stępień), malgorzata.przybylo@uj.edu.pl (M. Przybyło).

https://doi.org/10.1016/j.lfs.2018.06.026
Received 17 March 2018; Received in revised form 15 June 2018; Accepted 22 June 2018
Available online 27 June 2018
0024-3205/ © 2018 Elsevier Inc. All rights reserved.

Specific changes in glycosylation are considered the major hallmark of tumors [7–9]. *In vitro* studies on exosomes released by T-cell [10], cutaneous melanoma [10, 11], colon [10] and ovarian cancer cells [12, 13] showed the enrichment or depletion of specific glycan epitopes in comparison to the parental cell membranes. Major observations included the enrichment in high-mannose and complex type *N*-linked glycans as well as α2,6-linked sialic acid (SA) and poly-*N*-acetyllactosamine epitopes, along with the exclusion of terminal blood group A and B antigens, suggesting a significant role for glycosylation in exosomal protein sorting [10–13]. Glycosylation of EVs is also crucial for their interactions with recipient tumor cells and the exerted biological effect [14, 15].

The glycosylation of ectosome proteins released by tumor cells has not been explored yet. Therefore, studies on glycan composition of ectosomes might provide a new insight into the mechanisms of EVs action during tumor progression including glycan-mediated sorting of their specific cargo or the recognition and uptake by recipient cells. We used a panel of lectins to investigate specific glycosignatures of ectosomes released *in vitro* by two pairs of isogenic human CM cell lines. The obtained glycoprofiles were then compared in terms of disease stage (primary or metastatic origin of cell lines) and with the glycosylation pattern of the parental whole cell extracts and the cell membranes (Fig. 1).

2. Materials and methods

2.1. Materials

RPMI-1640 GlutaMAX™-I medium, fetal bovine serum (FBS) and Pierce Micro BCA Protein Assay Kit were purchased from Thermo Fisher Scientific (Waltham, Massachusetts, United States). Trypsin-EDTA solution, penicillin/streptomycin solution, protease and phosphatase inhibitor cocktails, extravidin-alkaline phosphatase (AP) conjugate, methyl-α-D-mannopiranoside, *N*-acetyl-D-galactosamine, mouse anti-human L1CAM monoclonal antibody (clone UJ127.11), mouse anti-human GAPDH polyclonal antibody, mouse anti-human β-actin monoclonal antibody (clone AT-15), goat anti-mouse IgG (Fab specific)-AP antibody and extravidin-FITC conjugate were obtained from Sigma-Aldrich (St. Louis, Missouri, United States). Rabbit anti-human Sirtuin-6 polyclonal antibody was obtained from LifeSpan BioSciences Inc. (Seattle, Washington, United States). Sheep anti-rabbit IgG-AP, mouse monoclonal anti-α5 integrin antibody (clone SAM-1) and mouse monoclonal anti-β1 integrin antibody (clone B3B11) were purchased from MerckMillipore (Darmstadt, Germany). Biotinylated lectins: *Phaseolus vulgaris* leukoagglutinin (PHA-L), *Phaseolus vulgaris* erythroagglutinin (PHA-E), *Sambucus nigra* agglutinin (SNA), *Maackia amurensis* agglutinin (MAA), *Galanthus nivalis* agglutinin (GNA) and *Aleuria aurantia* agglutinin (AAA) were purchased from Vector Laboratories Inc. (Burlingame, California, United States). Qproteome Cell Compartment Kit was purchased from Qiagen (Hilden, Germany).

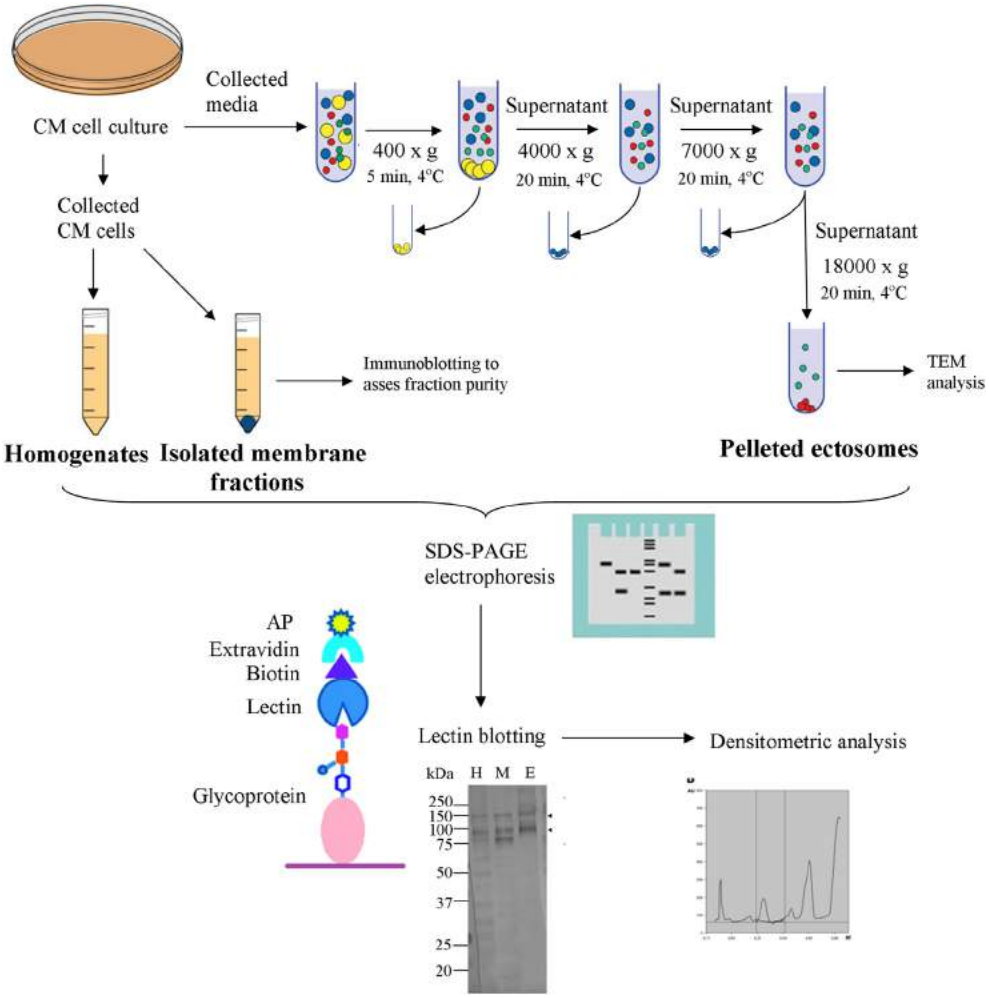

Fig. 1. Workflow scheme for lectin-blotting analysis of cutaneous melanoma cells, membrane fractions and ectosome samples. **AP**, alkaline phosphatase; **CM**, cutaneous melanoma; **E**, ectosomes; **H**, the whole cell extract; **M**, membrane fractions; **TEM**, transmission electron microscopy.

ApogeeMix reference beads were purchased from Apogee Flow Systems (Northwood, UK). All remaining chemicals were of analytical grade, commercially available.

2.2. Cell lines and cell culture conditions

Four cutaneous melanoma cell lines were obtained from the ESTDAB Melanoma Cell Bank (Tübingen, Germany). WM115 (primary CM) and WM266-4 (metastatic CM) cell lines originated from the same individual and represented radial/vertical growth phase and lymph node metastasis, respectively [16]. Primary WM793 cell line, representing vertical growth phase [17] and WM1205Lu, a highly metastatic variant of WM793 cells obtained from lung metastasis [18], were also used. All cell lines were maintained as previously described [19]. Briefly, all cell lines were maintained on 100 mm Petri dishes in RPMI 1640 medium with GlutaMAX-I, supplemented with 10% FBS, penicillin (100 unit/ml) and streptomycin (100 µg/ml). Cells were grown in monolayers in 5% CO_2 atmosphere at 37 °C in a humidified incubator and passage after reaching 80% of confluence.

2.3. Isolation of ectosomes

Sub-confluent cells were cultured for 24 h in serum-free RPMI-1640 GlutaMAX™-I medium supplemented with and antibiotics. Next conditioned media were collected and subjected to sequential centrifugation steps. After centrifugations at 400 ×*g* (5 min, 4 °C), 4000 ×*g* (20 min, 4 °C) and 7000 ×*g* (20 min, 4 °C), the remaining cells and cellular debris were pelleted and discarded. Supernatants were collected for ectosome isolation. After final centrifugation at 18000 ×*g* (20 min, 4 °C) ectosomes were pelleted and resuspended in ice cold PBS (Fig. 1).

2.4. Transmission electron microscopy (TEM)

Pelleted ectosomes were fixed with 2.5% glutaraldehyde in 0.1 M cacodylic buffer (CB) overnight at 4 °C, washed with 0.1 M CB, post-fixed in 1% osmium tetroxide/0.1 M CB solution, dehydrated by passing through a graded ethanol series, embedded in PolyBed 812 (epoxy resin) and polymerized for 48 h at 60 °C. Ultrathin sections were prepared with EM UC7 Leica ultramicrotome and collected on a copper mesh. The latter was covered with formvar film. Finally, the sections were contrasted with use of uranyl acetate and lead citrate. The sections were viewed on JEOL JEM 2100HT TEM at accelerating voltage of 80 kV. Diameter analysis was performed by means of the ImageJ software [20] after image binarization and using adaptive threshold settings.

2.5. Preparation of cell extracts

The cell extracts were prepared from cells after conditioned medium was collected. The cells were sonicated on ice in 50 mMTris/HCl buffer, pH 7.5, containing150 mM NaCl,2 mM EDTA, protease inhibitor cocktail (2 µl/100 µl), phosphatase inhibitor cocktail (1 µl/100 µl), 1 mM phenylmethylsulfonyl fluoride, 1 mM sodium fluoride and 5 mM tetrasodium pyrophosphate. Subsequently, Triton X-100 (final concentration 1%) and protamine sulfate (final concentration 0.3%) were added. The homogenates were then incubated for 30 min with shaking at 4 °C. Finally, the cell extracts were clarified by centrifugation at 18,000 ×*g* for 20 min at 4 °C and protein concentration was quantified with the use of the Micro BCA Protein Assay Kit.

2.6. Isolation of the membrane fractions

The membrane fractions of collected cells were obtained using the Qproteome Cell Compartment Kit and desalted *via* acetone precipitation according to the manufacturer's protocol. Protein concentration was quantified with the use of a Micro BCA Protein Assay Kit.

2.7. The membrane fraction purity assessment

For each cell line, the whole cell extract and the membrane fraction samples (70 µg of proteins) were separated by 10% SDS-PAGE in reducing condition, and electrotransferred to PVDF membrane. The purity of the membrane fraction was assessed with the use of anti-L1CAM (1:5000), anti-α_5 integrin subunit and anti-β_1 integrin subunit antibodies (1:5000) and the presence of the proteins specific for other subcellular fractions was excluded using anti-actin antibodies (1:10000) for the cytoskeletal fraction, GAPDH (1:4000) for the cytosolic fraction and sirtuin-6 (1:500) for the nuclear fraction. Suitable anti-mouse IgG-AP or anti-rabbit IgG-AP (1:4000) were used as a secondary antibody. Conjugated alkaline phosphatase was detected *via* NBT/BCIP staining.

2.8. Lectin blotting

Lectin dilutions (1:4000) were prepared with buffer 1 containing 1 mM $MgCl_2$, 1 mM $MnCl_2$ and 1 mM $CaCl_2$ dissolved in TBS (50 mM Tris/HCl, pH 7.5, 150 mM NaCl). Simultaneously, 1:4000 lectin dilutions were prepared with the addition of the competitive sugar or 0.2 M CH_3COOH (Table 1) and preincubated overnight. For each cell line and lectin, homogenates, the membrane fractions and ectosome samples containing 70 µg of protein were diluted 1:1 with 2× concentrate Laemmli sample buffer with 5% β-mercaptoethanol and separated by 10% SDS-PAGE, followed by transferred to PVDF membrane for 1 h at a constant voltage of 100 V with cooling. The blots were then blocked overnight in lectin blocking solution. Afterwards, membranes were washed twice with TBS/Tween (TBS containing 0.1% Tween 20) and once with buffer 1 and then incubated for 1 h with appropriate lectins. After triple wash with TBS/Tween, blots were incubated for 1 h with extravidin-AP. Next, membranes were washed three times with TBS/Tween and three times with TBS. The conjugated alkaline phosphatase was detected *via* NBT/BCIP staining. The dried membranes were photographed with UVtec camera and ScionImage software. The densitometric analysis of obtained bands was performed with a use UVmap V.99 software. After densitometric measurements areas under the peaks (expressed in arbitrary units) were compared to detect changes in the strength of lectin staining of a corresponding bands between membrane fractions and ectosome samples.

2.9. Flow cytometry

Cell surface glycosylation of CM cells and ectosomes was analyzed according to the method of Przybyło et al. [31] with minor

Table 1
Sugar-binding specificities of lectin used for lectin blotting studies and composition of blocking solutions.

Lectin	Lectin-specific glycan structures	Blocking solution
Aleuria aurantia agglutinin (AAA)	Fucα1,6GlcNAc-Asn Fucα1,2Galβ1,4GlcNAc- Galβ1,4(Fucα1,3)GlaNAc-	0.5 M L-(-)-fucose)
Galanthus nivalis agglutinin (GNA)	Manα1,2Man- Manα1,6Man- Manα1,3Man-	0.5 M methyl-α-D-mannopiranoside
Sambucus nigra agglutinin (SNA)	NeuAcα2,6Gal-	0.4 M CH_3COOH
Maackia amurensis agglutinin (MAA)	NeuAcα2,3Gal-	0.4 M CH_3COOH
Phaseolus vulgaris leukoagglutinin (PHA-L)	Galβ1,4GlcNAcβ1,6Manα- Galβ1,4GlcNAcβ1,2Manα- (β1,6-branched structures of *N*-glycans)	1 M *N*-acetyl-D-galactosamine
Phaseolus vulgaris erythroagglutinin (PHA-E)	Galβ1,4GlcNAcβ1,2Man (the bisecting GlcNAcβ1,4Man is essential)	1 M *N*-acetyl-D-galactosamine

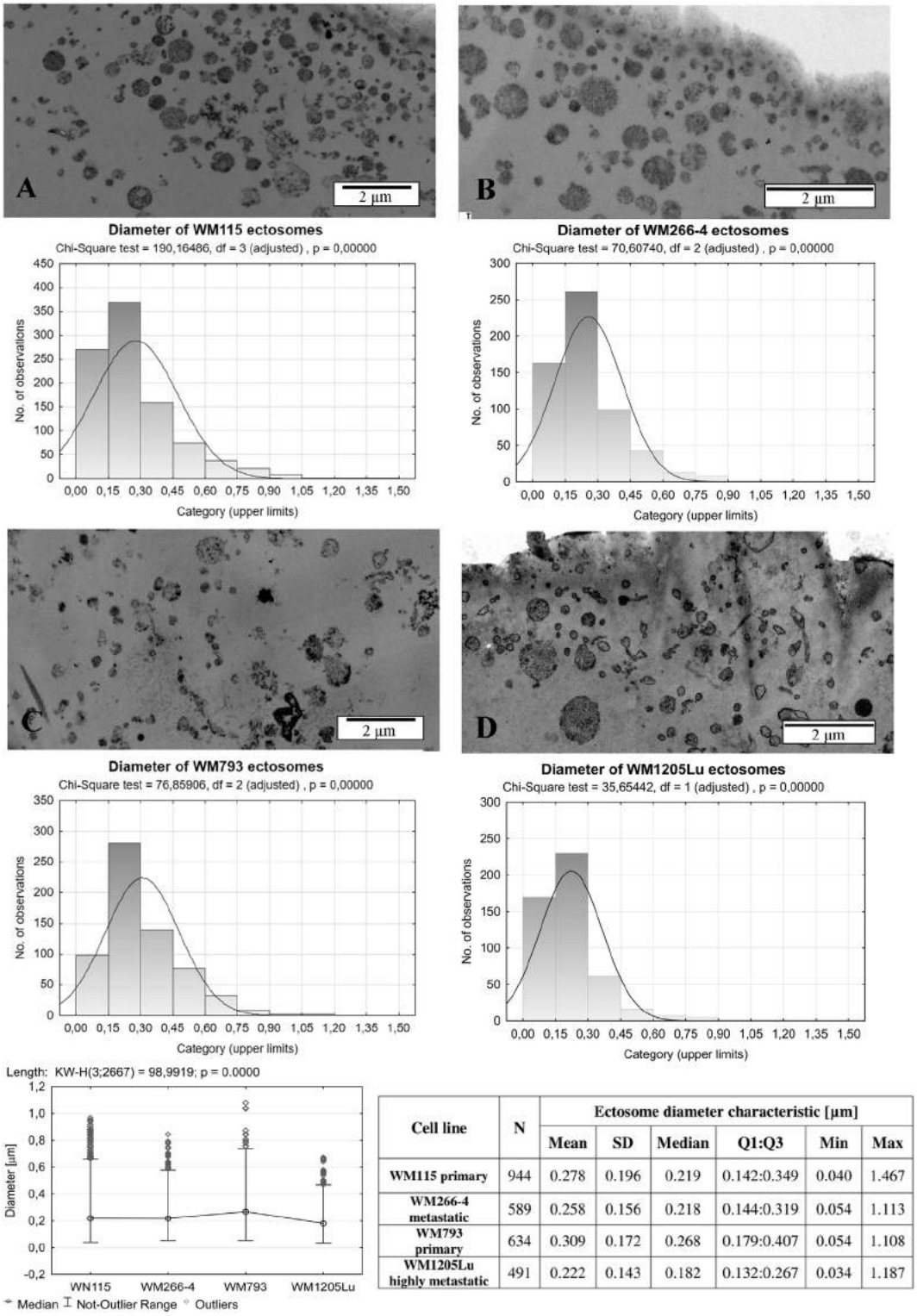

Cell line	N	Ectosome diameter characteristic [µm]					
		Mean	SD	Median	Q1:Q3	Min	Max
WM115 primary	944	0.278	0.196	0.219	0.142:0.349	0.040	1.467
WM266-4 metastatic	589	0.258	0.156	0.218	0.144:0.319	0.054	1.113
WM793 primary	634	0.309	0.172	0.268	0.179:0.407	0.054	1.108
WM1205Lu highly metastatic	491	0.222	0.143	0.182	0.132:0.267	0.034	1.187

Fig. 2. TEM analysis of ectosome isolates. **A**, ectosomes from WM115 cells; **B**, ectosomes from WM266-4 cells; **C**, ectosomes fromWM793 cells; **D**, ectosomes from WM1205Lu cells. Diameter distribution of N exosomes was analyzed. Mean (SD) and Median (Q1:Q2) are presented with outlined and mix-max values. Non-parametric test showed that WM793 ectosomes were significantly larger in size than others ($p < 0.0001$).

modifications. Briefly, cells ($7{,}5 \times 10^4$) and ectosomes (isolated from 10 ml of conditioned media *per* sample) incubated with biotinylated PHA-E, PHA-L, MAA, SNA, AAA and GNA lectins (20 µg/ml PBS) in for 45 min at 4° and washed with PBS. Subsequently, all samples were incubated with fluorescein isothiocyanate (FITC)-extravidin conjugate (25 µl/ml) under the same conditions and washed again. The assessment for cell fluorescence was done in a FACSCalibur flow cytometer (BD Biosciences, San Diego, CA) and a total of 10^4 cells were analyzed for each immunofluorescence profile. Ectosome samples were analyzed on Apogee A50 Micro flow cytometer (Apogee Flow Systems, Hemel Hempstead, UK) for 120 s with flow rate of 1,5 µl/min, sample volume set at 150 µl and sheath pressure at 150 mb. The trigger was set

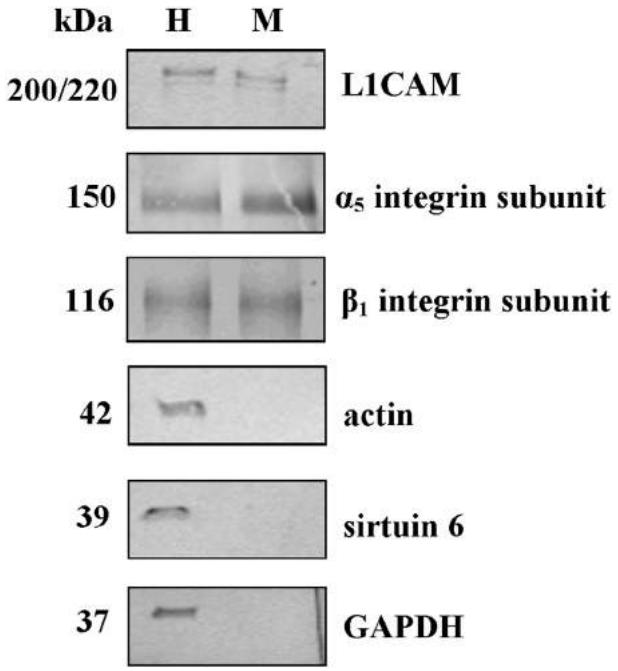

Fig. 3. Assessment of the membrane fraction purity. On-blot immunodetection of proteins representative for each subcellular fraction was performed for the whole cell extracts (**H**) and the membrane fractions (**M**) obtained from each CM cell line. Loading controls: anti-L1CAM, anti-α_5 integrin subunit and anti-β_1 integrin subunit (for the membrane fraction), anti-actin (for the cytoskeletal fraction), anti-sirtuin-6 (for the nuclear fraction), anti-GAPDH (for the cytosolic fraction). Representative results obtained for primary WM793 cells are shown. For other CM cell lines results were consistent.

on MALS detector with voltages 420 V, and on green fluorescent channel (488 Gn) with voltages 475 V on 488 nm laser. For daily calibration the reference beads composed of a mixture of 180 nm, 240 nm, 300 nm, 590 nm, 880 nm, and 1300 nm silica vesicles and 110-nm and 500-nm green fluorescent latex beads were used. For the analysis samples were diluted in order to obtain < 5000 events/s.

2.10. Statistical analyses

Statistica 12 (StatSoft®) tools were used for all data analyses and graph plotting Non-parametric Kruskal-Wallisone-way analysis of variance was used to compare ectosome diameter distribution. All other results are expressed as mean ± standard deviation of three independently carried out experiments. The significant differences between mean value were computed using one-way ANOVA and *post hoc* Tukey's test, and p-values < 0.05 were considered statistically significant. Classification and regression tree analysis was performed to predict which cell fraction (H – the whole cell extract, M – membrane fraction, E – ectosomes) had a specific protein band glycosylated in the most characteristic manner.

3. Results

3.1. Transmission electron microscopy of ectosome isolates

TEM analysis was done to validate the purity and effectiveness of ectosome isolation from the conditioned media *via* sequential centrifugation (Fig. 2). Ultrathin sections of ectosomes from each cell line contained extracellular vesicles, ranging approximately from 120 to 960 nm in diameter. The observed populations were rather heterogeneous and contaminated neither with intact cells nor with any cellular organelles. Extracellular vesicles smaller than 100 nm and larger than 1 μm in diameter were not found. The distribution of ectosome size was non-normal, with the median values typical for ectosome fractions. A non-parametric Kruskal-Wallis one-way analysis of variance

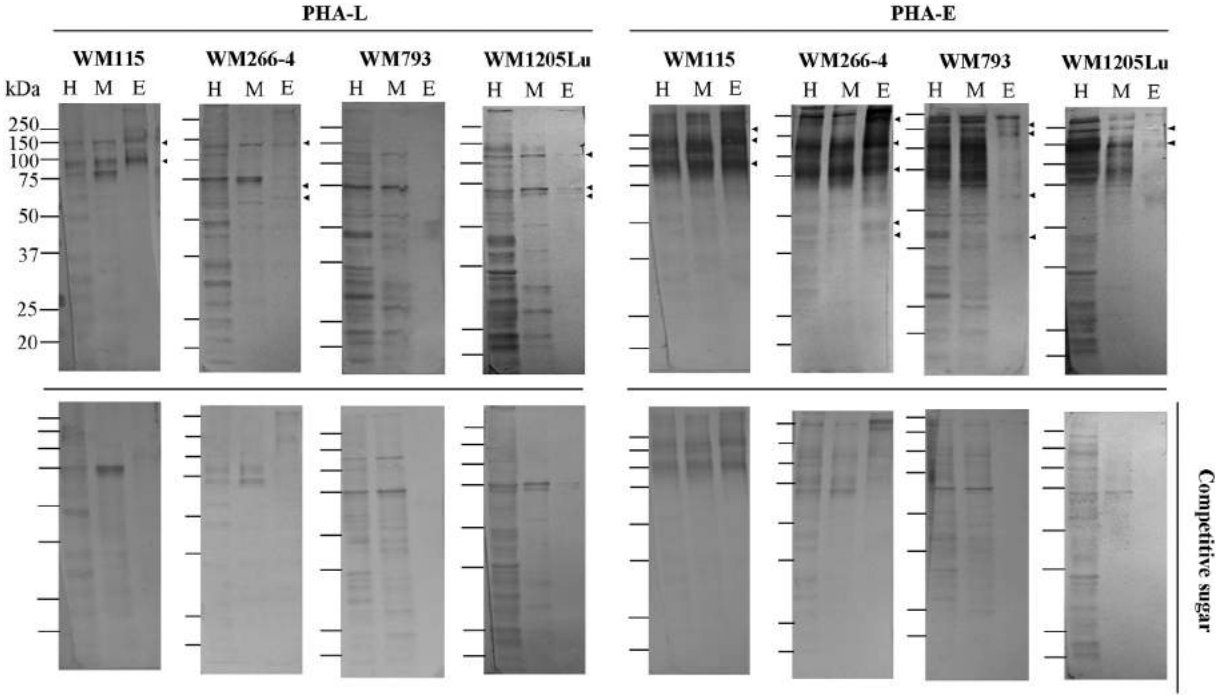

Fig. 4. Detection of glycoproteins possessing β1,6-branched tri- and/or tetraantennary complex type *N*-glycans (PHA-L-positive) and bisecting GlcNAc bound to the core mannose of complex type *N*-glycans (PHA-E-positive). Results of lectin blotting with PHA-L and PHA-E are shown in the upper panels and controls with the competitive sugars are shown in the lower panels. The major specific bands were indicated on the right with arrowheads. **H**, the whole cell extract; **M**, the membrane fraction; **E**, the ectosomal fraction.

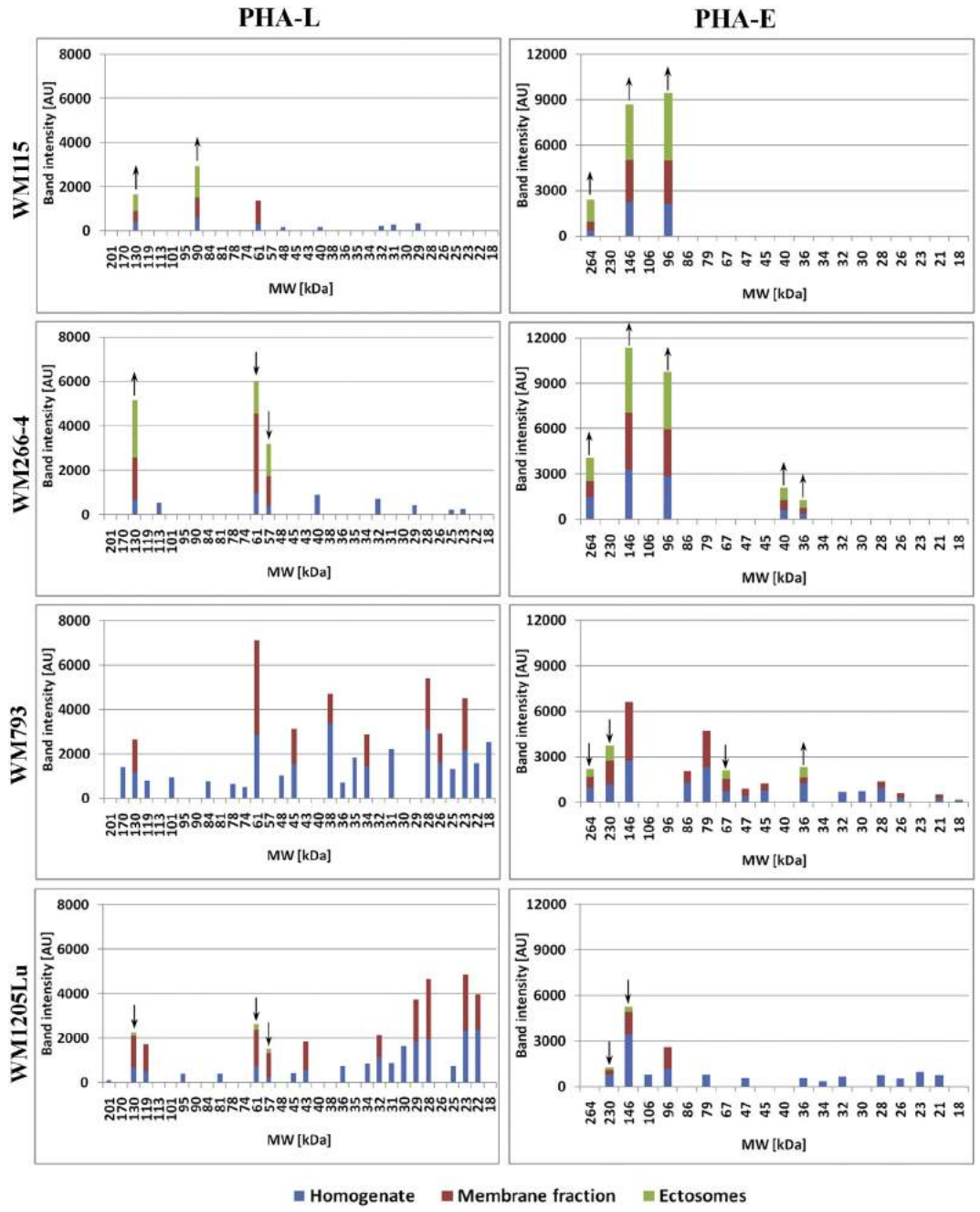

Fig. 5. Densitometric analysis of PHA-L- and PHA-E-positive bands. The intensity of detected bands was expressed in arbitrary units (AU) as a peak area on respective densitogram. Each bar represents the intensity of corresponding bands in the whole cell extracts, membrane fractions and ectosome samples from each CM cell line. ↑ and ↓ denote a significant enrichment or depletion, respectively, of a given glycoepitope in the ectosomal fraction (green) compared to membrane fraction (red). The values from control lectin blots with blocking solutions were subtracted beforehand. (For interpretation of the references to color in this figure legend, the reader is referred to the web version of this article.)

confirmed a significantly higher diameter (but still within the predefined range) for ectosomes isolated from WM793 cells. These data proved that the ectosome isolation protocol was standardized and did not cause any bias in ectosome purity.

3.2. Purity of isolated membrane fractions

The purity of the obtained samples was verified with the use of antibodies against proteins representative for each subcellular fraction (Fig. 3). L1CAM, a transmembrane cell adhesion molecule, was detected as a doublet with bands at MW of 200 and 220 kDa in the cell extracts and in the respective membrane fractions. Analogously, we confirm the presence of two subunits of transmembrane integrin receptor α_5 and β_1 in the cell extracts and in the respective membrane fractions. Actin, a major component of the cytoskeleton, was present only in the whole cell extracts and was detected as a band at MW of 42 kDa. Sirtuin-6, a stress responsive nuclear protein with ADP-ribosyl transferase and histone deacetylase activity, was detected only in the whole cell extracts at MW of 39 kDa. GAPDH was chosen as a loading control for the cytosolic fraction and detected in the whole cell extracts at MW of 37 kDa. Taken together, the isolated membrane fractions did not contain chosen proteins specific for other subcellular fractions, and, therefore, they were used for further analysis.

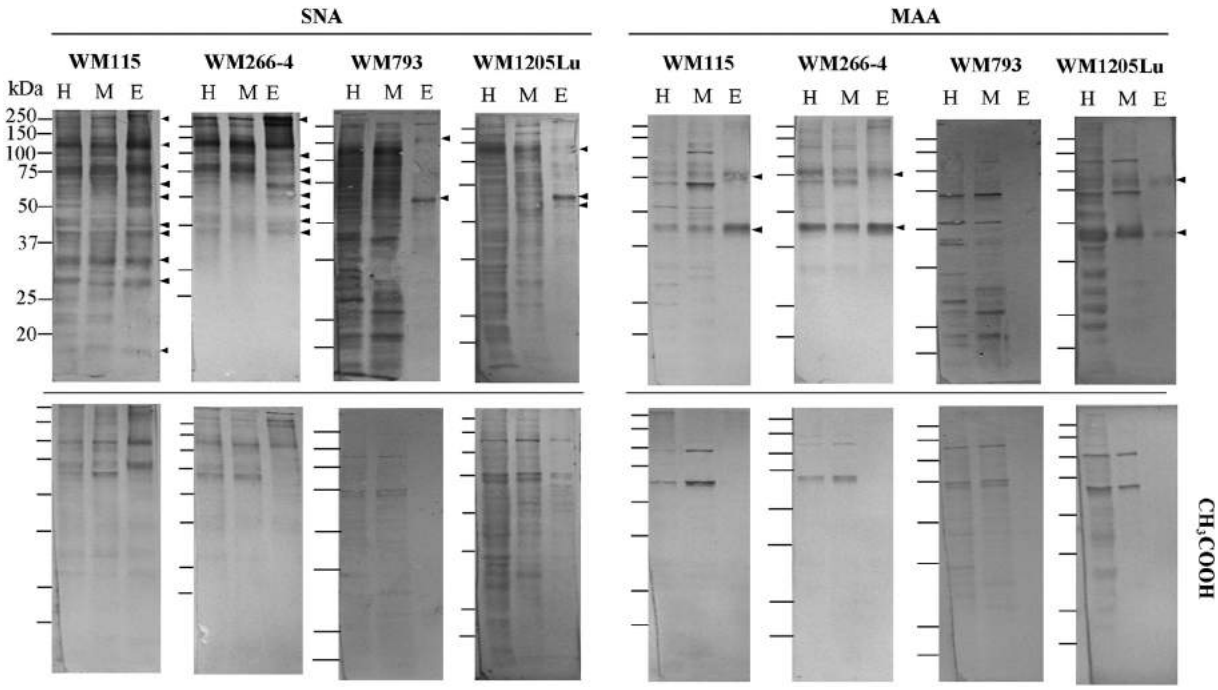

Fig. 6. Detection of glycoproteins carrying α2,6-linked (SNA-positive) and α2,3-linked (MAA-positive) SA. Results of lectin blotting with SNA and MAA are shown in the upper panels and controls with CH_3COOH are shown in the lower panels. The major specific bands were indicated on the right with arrowheads. **H**, the whole cell extract; **M**, the membrane fraction; **E**, the ectosomal fraction.

3.3. Specific glycosignatures of metastatic melanoma ectosomes

In the present study the whole cell extract, the membrane fraction and ectosomal proteins from four CM cell lines were analyzed by lectin blotting to investigate their glycosignatures. Reaction with PHA-L lectin (Figs. 4 and 5) confirmed the presence of β1,6-branched tri- and/or tetraantennary complex type *N*-glycans in the whole cell extract and the membrane fraction proteins. The isogenic cell lines (WM115 and WM266-4 as well as WM793 and WM1205Lu) showed similar PHA-L binding patterns. The number of PHA-L-positive bands was reduced in the membrane fractions, to a greater extent in the membrane fractions from WM115 and WM266-4 cells. In ectosomes either few or no PHA-L-positive bands were detected. PHA-L-positive band at MW of 130 kDa was present in ectosomal proteins obtained from WM115, WM266-4 and WM1205Lu cells, but absent in ectosomal proteins obtained from primary WM793 cells. Additionally, a band at MW of 90 kDa was detected in ectosomal proteins obtained from WM115 cells, but it did not appear in any other ectosome samples. Lectin blots for two metastatic cell lines (WM266-4 and WM1205Lu) revealed a pair of corresponding bands at MW of 57 and 61 kDa in ectosome samples.

PHA-E lectin was used to detect proteins possessing bisecting GlcNAc in their complex type *N*-glycans (Figs. 4 and 5). In the whole cell extracts, membrane fractions and ectosomes from WM115 and WM266-4 cells strong positive reactions were detected for protein bands with MW above 75 kDa. Moreover, PHA-E-positive bands were enriched in ectosomes (compared to homogenates and the membrane fractions), suggesting that proteins possessing glycan structures with bisecting GlcNAc could be preferentially recruited into ectosomes derived from WM115 and WM266-4 cells. Such a phenomenon was not observed in case of the samples obtained from WM793 and WM1205Lu cells. Despite the presence of multiple PHA-E-positive proteins bands in the whole cell extracts and the membrane fractions, only few weak PHA-E-positive bands were detected in the ectosome samples.

Two lectins, *i.e.* SNA and MAA, were used to detect proteins carrying α2,6- and α2,3-linked SA, respectively (Figs. 6 and 7). Reaction with SNA revealed similar binding patterns in related cell lines (WM115 and WM266–4 as well as WM793 and WM1205Lu) and the enrichment of several bands in the ectosomal fraction obtained from WM115 and WM266-4 cells was stated. In the ectosome samples from WM793 and WM1205Lu cells only two bands were detected. Moreover, there were two SNA-positive bands at MW of 56 and 122 kDa that were detected in all ectosomal fractions. Reaction with MAA revealed that the whole cell extracts and the membrane fractions obtained from all studied cell lines contained less bands possessing α2,3-linked SA than carrying α2,6-linked SA (reaction with SNA). In the ectosome samples obtained from three cells lines (WM115, WM266-4 and WM1205Lu) two corresponding bands at MW of 46 kDa and 89 kDa were detected, however there were no such MAA-positive glycoproteins in the ectosome samples from WM793 cells.

Positive reaction with GNA lectin confirmed the presence of proteins having high-mannose and/or hybrid type oligosaccharides, both in the whole cell extracts and the membrane fractions from all cell lines (Figs. 8 and 9). Mannose-rich glycoproteins, however, were not commonly sorted into ectosomes, apart from one band detected with GNA at MW of 78 kDa in each cell line.

The presence of proteins possessing fucose residues was revealed by the reaction with AAA lectin (Figs. 8 and 9). AAA binds fucose with α1,6-linkage to the proximal GlcNAc residue as well as Galβ1,4(Fucα1,3)GlcNAc sequence. In homogenates and the membrane fractions obtained from two primary melanoma cell lines (WM115 and WM793) strong reaction was observed with only two specific bands as revealed by control with the competitive sugar. In two metastatic cell lines (WM266-4 and WM1205Lu) AAA binding to protein cell extract and the membrane glycoproteins was reduced to bands above 70 kDa. In case of ectosomal proteins, related WM115 and WM266-4 cell lines had the same two AAA-positive bands (at MW of 85 and 149 kDa) with stronger intensity compared to corresponding bands in the whole cell extracts and the membrane fractions. Those glycoproteins enriched with fucose could be preferentially recruited into ectosomes from WM115 and WM266-4 cells, however, it was not observed in case of ectosomes derived from two remaining cell lines (WM793 and WM1205Lu), where significantly fainter bands were detected.

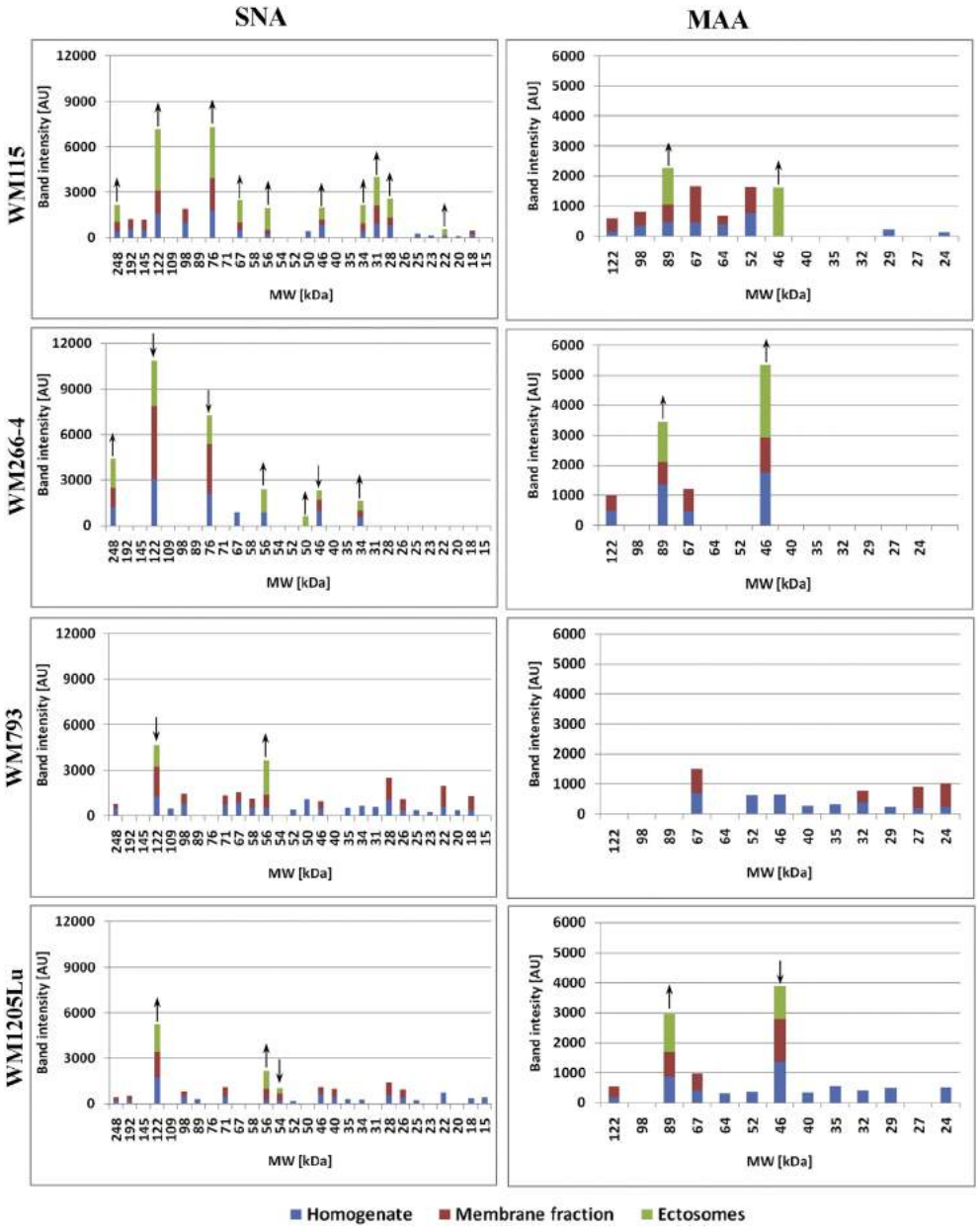

Fig. 7. Densitometric analysis of SNA- and MAA-positive bands. The intensity of detected bands was expressed in arbitrary units (AU) as a peak area on respective densitogram. Each bar represents the intensity of corresponding bands in the whole cell extracts, membrane fractions and ectosome samples from each CM cell line. ↑ and ↓ denote a significant enrichment or depletion, respectively, of a given glycoepitope in the ectosomal fraction (green) compared to membrane fraction (red). The values from control lectin blots with blocking solutions were subtracted beforehand. (For interpretation of the references to color in this figure legend, the reader is referred to the web version of this article.)

In order to reveal the specific glycosylation band(s) to predict a cell fraction, the classification and regression tree method was used (Fig. 10). The classification tree plots discriminated three cell fractions from four CM cell lines to find a specific protein band of a given MW (kDa), which was up- or down-glycosylated. For each CM line, if the protein band of 56 kDa is carrying more α2,6-linked SA (positive reaction with SNA), with bar intensity over 1056.5 AU, this fraction should be considered as the ectosomal fraction. Similarly, if the 67 kDa protein band shows the significant down-glycosylation for α2,3-linked SA (positive reaction with MAA) with a cut-off under 196.5 AU, the analyzed fraction should be considered as ectosomal in each of the CM cell lines. In addition, down-glycosylation with mannose residues (positive reaction with GNA) in the 150 kDa protein band predicts the ectosomal fraction (cut-off 327.5 AU). For bisecting GlcNAc in the complex type of *N*-glycans (positive reaction with PHA-E), the protein band of 146 kDa down-glycosylation in the E fraction was shown at the cut-off at 904 AU, but this was only confirmed for two CM lines (WM793 and WM1205Lu).

3.4. Surface expression of glycan epitopes on CM cells and CM-derived ectosomes

In order to verify to what extend the revealed enrichment or depletion of specific glycoepitopes in CM-derived ectosomes in comparison to the parental CM cell membranes is related to the surface (plasma membrane-associated) and/or intracellular glycoproteins flow cytometry was used. By applying the same panel of lectins as in lectin blotting studies (*i.e.* AAA, GNA, SNA, MAA, PHA-E and PHA-L) the comparison of the surface glycosylation of CM cells and CM-derived ectosomes was performed.

It was found that > 95% of CM cells possessed α2,3-linked SA, fucose residues, bisecting GlcNAc in complex type *N*-glycans, as well as β1,6-branched tri- and/or tetraantennary complex type *N*-glycans as revealed by positive staining with MAA, AAA, PHA-E and PHA-L, respectively (Fig. 11A and B). Regarding the presence of α2,6-linked SA (positive staining with SNA) on the cell surface, a significant increase in the percentage of cells having such moiety was revealed for metastatic cell lines (WM266-4 and WM1205Lu) compared to their isogenic cells

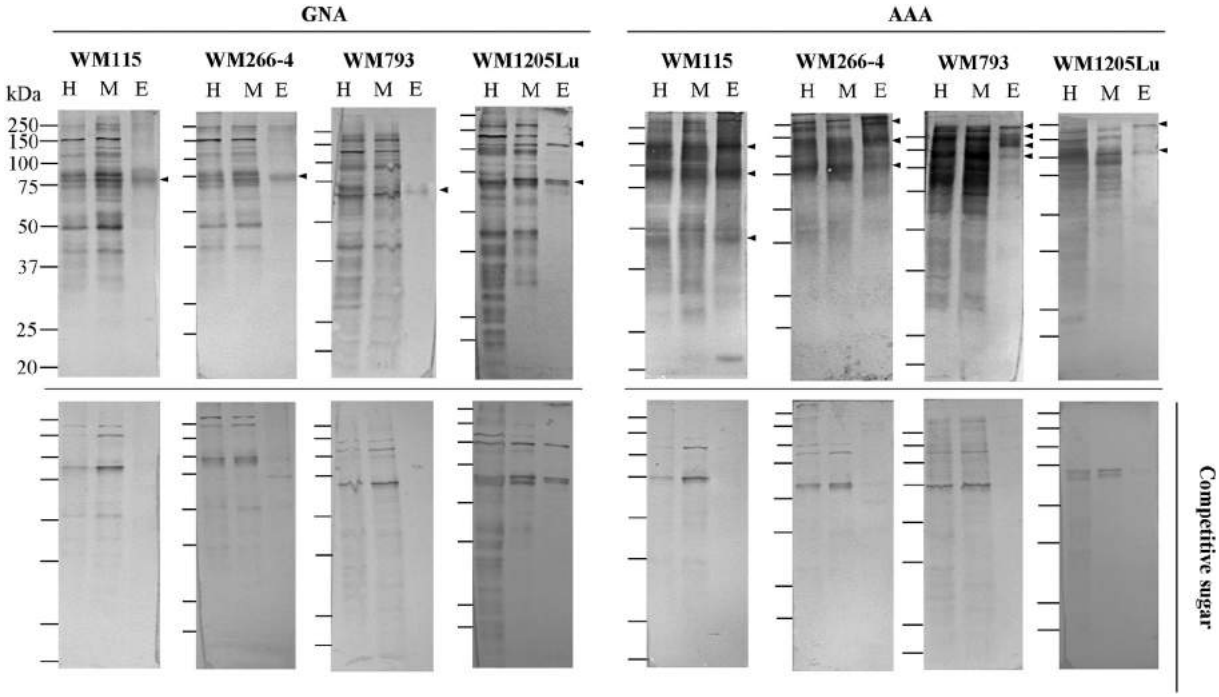

Fig. 8. Detection of glycoproteins having mannose (GNA-positive) and fucose (AAA-positive) residues. Results of lectin blotting with GNA and AAA are shown in the upper panels and controls with the competitive sugars are shown in the lower panels. The major specific bands were indicated on the right with arrowheads. **H**, the whole cell extract, **M**, the membrane fraction, **E**, the ectosomal fraction.

lines of primary origin (WM115 and WM793) - 99.8% and 99.7% *versus* 35.3% and 68.4%, respectively (Fig. 11A and B). Similarly, reaction with GNA revealed the higher percentage of cells bearing mannose residues in case of metastatic cell lines, however, the number of GNA-positive cells was much smaller than in case of staining with other lectins (Fig. 11A and B). Although the substantial differences in the percentage of positive cells among studied CM cell lines were observed only in case of SNA and GNA staining (Fig. 11A and B), the measurement of relative fluorescence intensity (RFI) revealed the greater diversity related to relative amount of given glycoepitopes on the cell surface (Fig. 11C). Complex type *N*-glycans with bisecting GlcNAc (PHA-E staining), β1,6-branched *N*-glycans (PHA-L staining), α2,3- and α2,6-linked SA (MAA and SNA staining, respectively) were more abundantly present on the cell surface of metastatic (WM266-4 and WM1205Lu) cells compared to the isogenic primary (WM115 and WM793) cell lines. Regarding AAA staining similar observation was made only for WM155 and 266-4 cells, while the second pair of isogenic cell lines showed opposite tendency. Finally, despite the higher percentage of GNA-positive cells in case of metastatic cell lines, higher RFI was stated for the isogenic primary cells lines.

Considering CM-derived ectosomes, the percentage of lectin-positive vesicles was highly decreased in comparison to the analogous staining of parental CM cells (Fig. 12A and B). It was found that ectosomes released by WM793 cells were to the greater extend the carriers of the studied glycan epitopes with the exception of having bisecting GlcNAc in complex type *N*-glycans on their surface (Fig. 12A and B). Furthermore, for almost each staining (excluding GNA and SNA staining of WM115 and WM266–4 cells) the percentage of lectin-stained ectosomes was significantly higher for primary CM-derived ectosomes compared to ectosomes derived from isogenic cells lines of metastatic origin (Fig. 12A and B). Regarding RFI, CM-derived ectosomes showed opposite tendency relative to the cells of their origin. Except for MAA and AAA staining for WM115- and WM266-4-derived ectosomes, higher RFI values were measured for ectosomes derived from primary CM cell lines in comparison to ectosomes derived from isogenic metastatic cell lines (Fig. 12C). Additionally, higher RFI values corresponded with higher percentage of lectin-stained ectosomes. Judging by RFI, CM cells and CM-derived ectosomes were stained by MAA and GNA to the smallest extend (Figs. 11C and 12C), however, this values cannot be compared directly, because two different types of flow cytometer were used for analysis of surface glycosylation.

4. Discussion

4.1. Glycan epitopes as a potential signal for ectosomal protein sorting

In the present study we showed that ectosomes have specific glycosignatures in comparison to their parental cell membrane fractions. Our findings are in line with previous reports showing characteristic changes (enrichment/depletion) in specific glycan structures in exosomes released *in vitro* [10–13]. The mechanisms by which proteins are targeted to ectosomes are not fully understood. Glycan-based protein sorting to EVs might be related to the glycan moieties and constitute the alternative to endosomal sorting complexes required for transport (ESCRT). ESCRT is known to be only involved in multivesicular bodies formation during biogenesis of exosomes [1, 2], what makes glycan-based sorting the first potential mechanism to be studied in case of ectosomes.

It has been hypothesized [13] that glycoproteins may interact with intracellular lectins such as galectins, which promote their specific sorting into exosomes or ectosomes. Galectin-3 [10, 13], galectin-4 [10] and galectin-5 [22] have been detected in EVs produced by different cells (carcinoma or macrophages). Galectin-3 binding protein *i.e.* lectin galactoside-binding soluble 3-binding protein (LGALS3BP) and another galectin-related protein (LGALSL) have been detected in exosomes derived from carcinoma cells, semen or activated platelets [12, 23, 24]. Moreover, galectin-5 has been proposed to modulate the amount of lysosome-associated membrane protein 2 (Lamp2), in exosomes during reticulocyte maturation [22]. Whether this mechanism involves a previous enrichment of particular membrane domains with specific glycan structures and/or glycoprotein oligomerization remains unclear and needs to be determined in further studies.

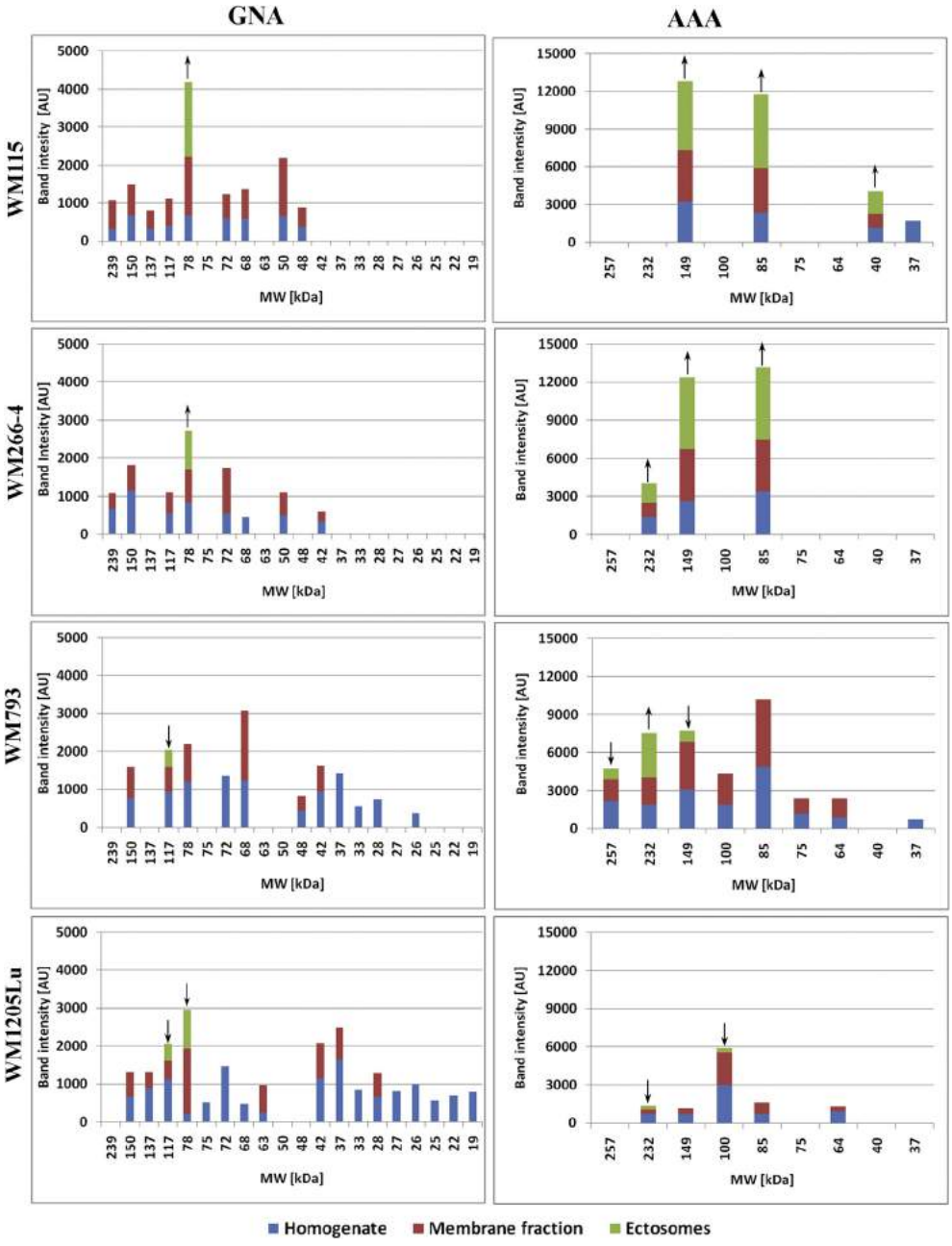

Fig. 9. Densitometric analysis of GNA- and AAA-positive bands. The intensity of detected bands was expressed in arbitrary units (AU) as a peak area on respective densitogram. Each bar represents the intensity of corresponding bands in the whole cell extracts, membrane fractions and ectosome samples from each CM cell line. ↑ and ↓ denote a significant enrichment or depletion, respectively, of a given glycoepitope in the ectosomal fraction (green) compared to membrane fraction (red). The values from control lectin blots with blocking solutions were subtracted beforehand. (For interpretation of the references to color in this figure legend, the reader is referred to the web version of this article.)

Regarding glycan structures that would significantly promote protein incorporation into exosomes, complex type *N*-glycans are so far the most widely studied. The treatment of OVMz cells with kifunensine, which prevents the processing of high-mannose to complex type *N*-glycans, decreased the levels of several *N*-linked glycoproteins (such as CD63, LGALS3BP, L1CAM) in EVs, whereas the same effect on the non-glycosylated protein annexin-I was not observed [13]. Similarly, the α-mannosidase I inhibitor, deoxymannojirimycin, decreased the level of glycoprotein EWI-2 in exosomes, and did not affect its expression on the cell surface [11]. Other major findings from that study were exosome enrichment in high-mannose glycans, poly-*N*-acetyllactosamine structures and α2,6-linked SA, however none of those observations have been confirmed in ectosomes thus far.

Our results indicate that glycan-based sorting of ectosomal proteins might depend on the cell origin, since similar lectin binding patterns were observed on blots for isogenic CM cell lines (WM115 and WM266-4 as well as WM793 and WM1205Lu). The enrichment mainly with glycoproteins having fucose moieties and complex *N*-glycans with bisecting GlcNAc in ectosomes derived from WM115 and WM266-4 cells was revealed. However, such observation was not stated for the samples from WM793 and WM1205Lu cell lines, where despite the presence of multiple PHA-E-and AAA-positive glycoproteins bands in the whole cell extracts and the membrane fractions, in ectosomes only few specific bands were detected. SNA-, MAA- and GNA-positive bands were detected at the same MW values in ectosomes derived from at least three CM cell lines. It suggests that a more conservative sorting mechanism in terms of sialoglycoproteins with α2,3-and α2,6-linked SA and high-mannose type *N*-glycans could occur. It is also important to notice that each glycoprotein band detected in ectosomes was also present in the membrane fractions.

Using flow cytometry analogous glycoepitopes on the surface of CM cells and CM-derived ectosomes were identified by the same panel of lectins. Such approach has never been applied in studies on EV glycosylation before, but is well justified by the mechanism of ectosome biogenesis that involves direct shedding of vesicles from the plasma membrane. The percentage of lectin-stained ectosomes was generally

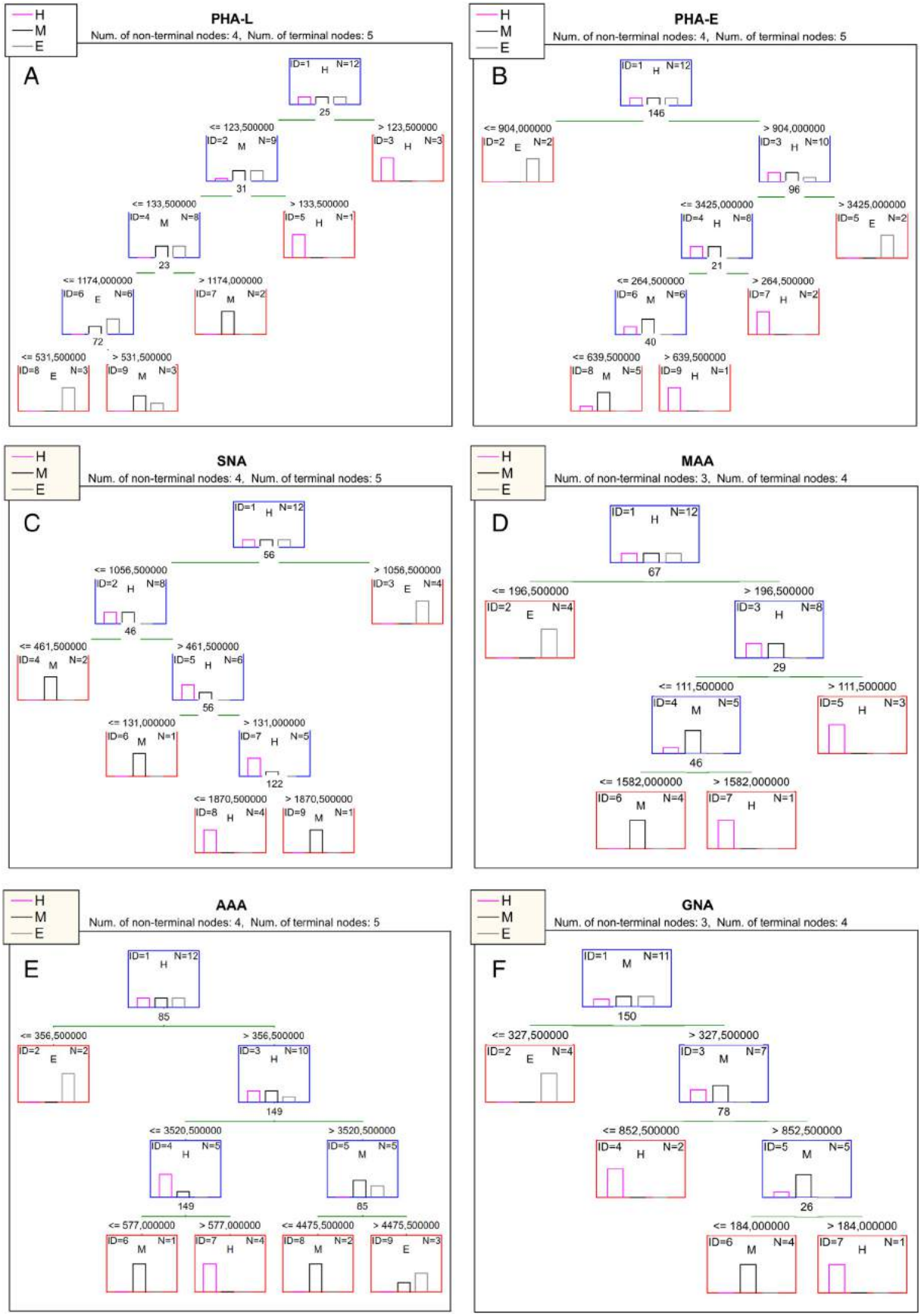

Fig. 10. Classification and regression trees for the cell fraction prediction from each cutaneous melanoma cell line with respect to the glycosylation profile. The most significant aspect for the ectosomal fraction prediction is SNA up-glycosylation of the 56 kDa protein band and down-glycosylation of 67 kDa (MAA-positive) and 150 kDa (GNA-positive) protein bands ($N = 4$). For other glycosylation residues (PHA-E-, PHA-L-, AAA-positive) the number of predicted cell lines is < 4. **H**, the whole cell extract; **M**, the membrane fraction; **E**, the ectosomal fraction.

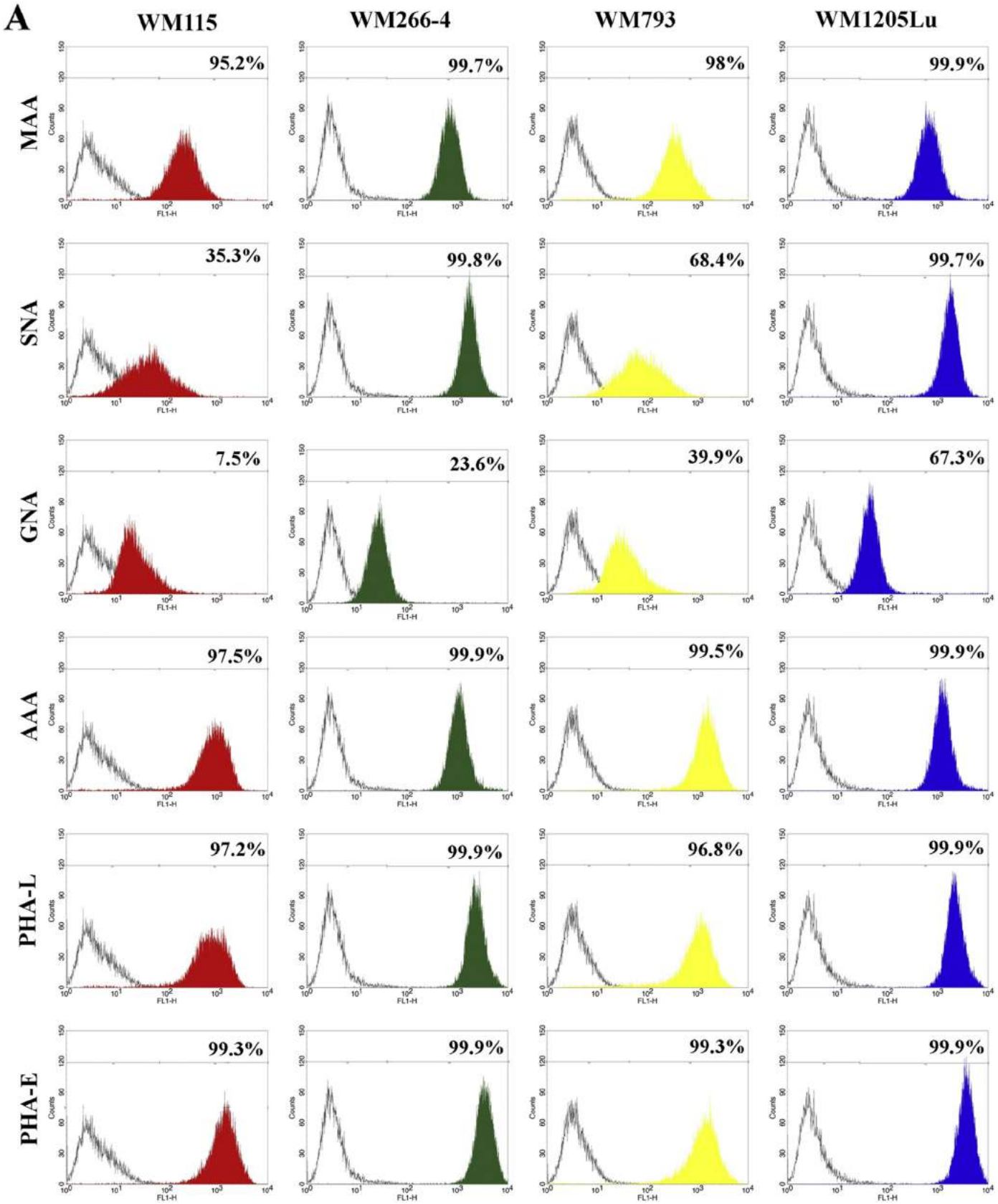

Fig. 11. Flow cytometry analysis of surface glycosylation of CM cells. **A**. Histograms for MAA-, SNA-, GNA-, AAA-, PHA-E- and PHA-L-positive cells. Colored areas represent stainings with a panel of six lectins, while open histograms represent background fluorescence of unspecific binding of FITC-extravidin. The X axis shows log fluorescence intensity, Y axis shows the number of events. **B**. Diagram showing the percentage of positive cells in each staining. **C**. Diagram showing the relative fluorescence intensity (RFI) for each staining. * - denotes statistically significant differences.

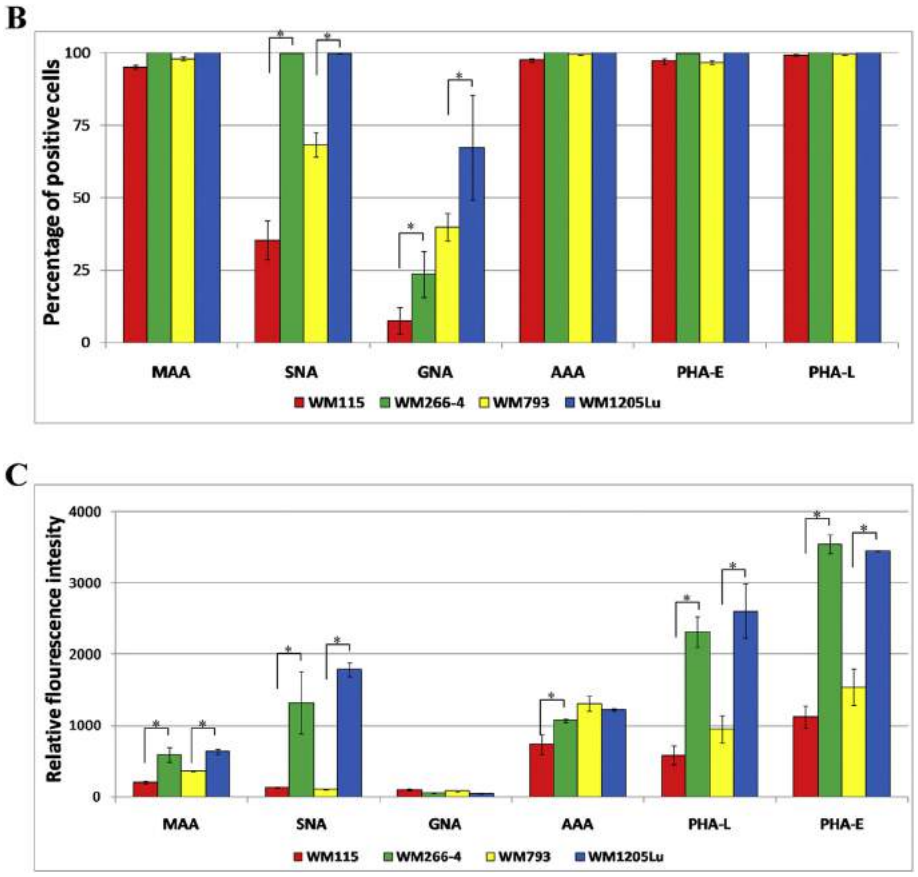

Fig. 11. (*continued*)

decreased in comparison to the analogous staining of the cell surface of CM cells. This finding once again supported the hypothesis that ectosomes were derived from particular regions of the cell membranes, because the molecular composition of the surface glycoconjugates differed markedly between the analyzed samples (the cell surface *versus* the ectosome surface). Due to the fact that two types of flow cytometers were used for measurements and the analyzed objects have different size range, it is not possible to directly compare the obtained RFI values for CM cells and CM-derived ectosomes as well as to identify the glycoepitopes that would be enriched in ectosomes based solely on flow cytometric data. Nevertheless, RFI values for CM-derived ectosomes still revealed the abundance of α2,6-linked SA, fucose, complex type *N*-glycans with bisecting GlcNAc and β1,6-branched *N*-glycans on their surface. Considering both percentages and RFI values it should be assumed that the enrichment in the amount of certain glycoepitopes revealed by lectin blotting studies concerned rather glycoconjugates that were sorted into the interior of ectosome than glycoconjugates present in its membrane.

4.2. Glycoconjugates of cutaneous melanoma ectosomes and cancer-associated epitopes

The changes in glycosylation are being increasingly studied in cancer, where neoglycoepitopes are associated with tumor progression and often used as disease biomarkers [25]. Major alterations to the cell surface glycosylation may be reflected on the surface of EVs, therefore their accessibility in different body fluids holds a great promise towards the development of new diagnostic and prognostic strategies [26].

Glycans play a fundamental role during tumor cell dissociation and invasion, mainly by interfering with intercellular signaling and cell-cell adhesion. An increased number of β1,6-branched *N*-glycan structures generally impairs cell adhesion and promotes tumor cell invasion. These β1,6-branched structures can be further extended, and terminal sialylation interferes with cell–extracellular matrix interactions, promoting a more migratory and invasive phenotype. On the other hand, the presence of *N*-glycans with bisecting GlcNAc may lead to protein stability and suppression of tumor progression [27, 28].

It has been demonstrated that higher expression of complex type β1,6-branched *N*-glycans may contribute to higher potential of primary (FM-55-P, IGR-39) CM cells to migrate on fibronectin and their weaker binding to extracellular matrix proteins [29–31]. Moreover, it has been shown that CM transition from the vertical growth phase to the metastatic stage was accompanied by elevated β1,6-branching of the cell surface *N*-glycoproteins, including α3β1 and α5β1integrins, which influenced melanoma cell migration potential [32]. Regarding ectosomal proteins, in the present study only few PHA-L-positive bands were detected by lectin blotting, however reaction with PHA-E showed a significant enrichment of vesicular content with bisecting GlcNAc structures in WM115- and WM266-derived ectosomes. Therefore, the release of glycoproteins with bisecting GlcNAc *via* ectosomes might be a potential mechanism that allows cancer cells to retain their metastatic potential.

Major changes in the level of sialylation and fucosylation of glycoproteins are also associated with cancer and are under constant evaluation as diagnostic and therapeutic targets. The fucosylated and sialylated structures often form the sialylated Lewis determinants present in *O*-glycans and *N*-glycans that participate in cell adhesion events underlying the formation of metastases *via* interaction with selectins [25, 26]. In the previous studies, the significance of sialylated derivatives on the CM cell surface was evaluated [21]. It was found that melanoma progression from the radial growth phase to the metastatic stage was associated with the elevated expression of α2,3-linked SA on the cell surface of the studied melanoma cells. These epitopes were able to modulate melanoma cell interaction with fibronectin. In the present

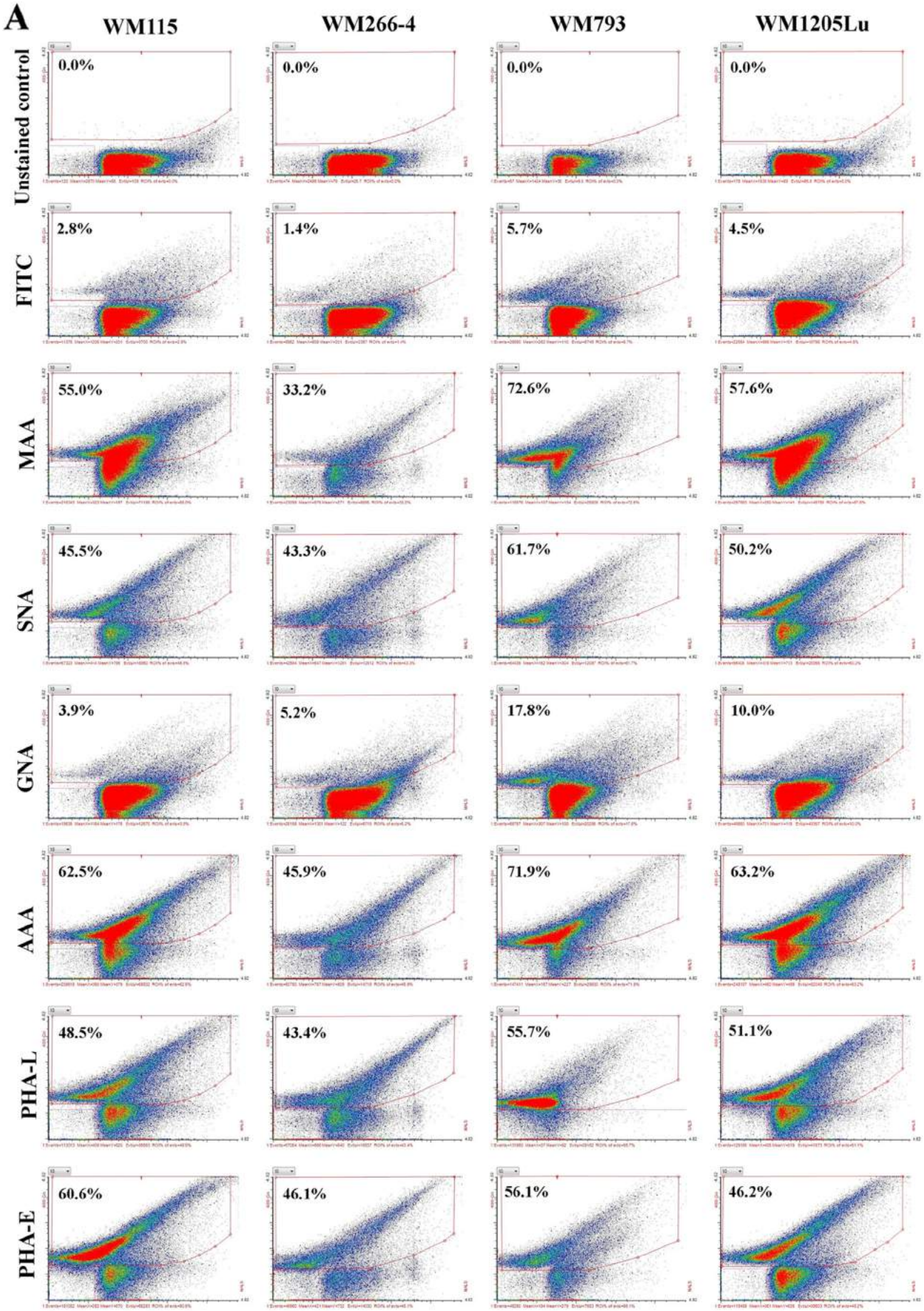

(caption on next page)

Fig. 12. Flow cytometry analysis of surface glycosylation of CM ectosomes. **A**. Dot plots for MAA-, SNA-, GNA-, AAA-, PHA-E- and PHA-L-positive ectosomes. Results for unstained control and control secondary extravidin-FITC conjugate staining are also provided. The X axis shows values obtained at medium angle light scatter (MALS), Y axis shows log fluorescence intensity measured on 488Gn laser. The corresponding histograms are presented in supplementary data. **B**. Diagram showing the percentage of positive ectosomes in each staining calculated by the subtraction of the value for the unspecific binding (secondary FITC-extravidin staining) from the raw value for each lectin staining. **C**. Diagram showing the relative fluorescence intensity (RFI) for each staining. * - denotes statistically significant differences.

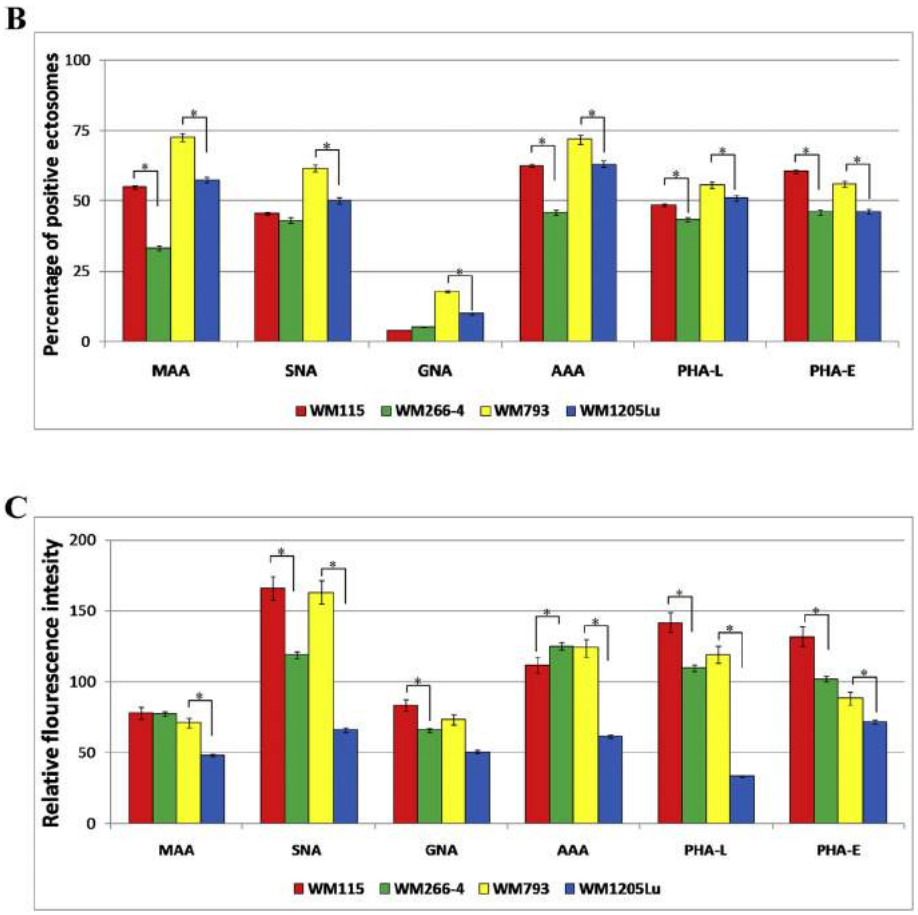

Fig. 12. (*continued*)

study, the enrichment of several sialoglycoprotein bands with α2,3- and α2,6-linked SA in ectosomes derived from CM cell lines was shown using lectin blotting. Moreover, glycoproteins enriched with fucose residues were preferentially recruited into ectosomes derived from WM115 and WM266-4 cells. Nevertheless, no significant differences between related primary and metastatic cell lines that would reflect the changes in total glycoprotein sialylation and/or fucosylation during disease progression were observed.

In particular cell surface glycosylation promote invasive behavior of tumor cells and may be essential for interactions between ectosomes and recipient cells, including mutual recognition or fusion. Since lectin blotting allowed the analysis of total protein glycosylation, flow cytometry was used to evaluate alterations in glycosylation of the cell and the ectosome surfaces. We showed that tumor-associated epitopes discussed above were abundantly present on the surface of CM-derived ectosomes. However, the percentage of lectin-stained ectosomes was generally smaller in comparison to the analogously stained CM cells suggesting some degree of retention of possibly tumor-promoting glycoepitopes by CM cells. For almost each lectin (except GNA) the percentage of stained ectosomes and RFI values were higher for ectosome released by primary CM cell lines and that increased (relatively to metastatic CM-derived ectosomes) surface glycosylation of ectosomes derived from primary CM cells might be a way by which primary CM cells prepare pre-metastatic niches through glycan-mediated uptake of ectosomes by recipient cells. It has been shown that niche formation is directed by integrin present on the exosome surface [33], what provides a new insight into the ability of certain tumors to metastasize to selected organs. It is well-established that integrins play a central role in malignancy and several studies have reported the control of integrin activation by its glycosylation status [27, 34–37]. Thus, a concerted effort is needed to characterize glycan content of ectosomes in order to explore the potential of ectosome glycosylation to manipulate cargo protein requirement or providing novel targeting strategies as well as diagnostic and therapeutic targets.

5. Conclusion

Our data supports recent findings suggesting that EVs derive from particular regions of the cell membrane and thus they contain a unique glycan composition. If proven correct, hypothesis that glycan-based protein sorting is a major mechanism for protein incorporation into EVs might provide new means to control vesicular content and have possible clinical implications. For further analysis of the glycan structures present in ectosomes high resolution techniques (*e.g.* MALDI-TOF MS, HPLC-MS, UPLC) should be used in the future. Also, functional studies and the use of glycosylation inhibitors or knockout/transfection of enzymes engaged in glycosylation are needed to establish the precise role of glycoepitopes in recognition and uptake of ectosomes by

recipient cells, protein recruitment into ectosomes *etc.* Moreover, exploring whether disease-associated glycoforms are enriched in EVs isolated from different body fluids will probably became a subject of future in-depth studies and may allow to develop novel biomarkers of CM.

Abbreviations

AAA	*Aleuria aurantia* agglutinin
AP	alkaline phosphatase
BCIP	5-bromo-4-chloro-3-indolyl-phosphate
CM	cutaneous melanoma
ESCRT	endosomal sorting complexes required for transport
EVs	extracellular vesicles
FBS	fetal bovine serum
GAPDH	glyceraldehyde 3-phosphate dehydrogenase
GNA	*Galanthus nivalis* agglutinin
L1CAM	L1 cell adhesion molecule
LGALS3BP	lectingalactoside-binding soluble 3-binding protein
MAA	*Maackia amurensis* agglutinin
NBT	4-nitro blue tetrazolium chloride
PHA-L	*Phaseolus vulgaris* leukoagglutinin
PHA-E	*Phaseolus vulgaris* erythroagglutinin
SA	sialic acids
SNA	*Sambucus nigra* agglutinin
TBS	Tris-buffered saline
TEM	transmission electron microscopy
TEVs	tumor-derived extracellular vesicles

Conflict of interest

The authors declare no conflict of interest.

Acknowledgement

This work was supported by grants from the Polish National Science Centre (2013/11/B/NZ4/04315) and from the Jagiellonian University in Kraków (K/DSC/003978 and K/ZDS/007347). We would like to thank the Department of Cell Biology and Imaging of the Institute of Zoology and Biomedical Research for the access to TEM.

Appendix A. Supplementary data

Figures showing calibration dot plots (Fig. S1) and cumulative histograms of lectin staining of CM-derived ectosomes (Fig. S2) obtained from Apogee flow cytometer. Supplementary data to this article can be found online at [doi:https://doi.org/10.1016/j.lfs.2018.06.026].

References

[1] G. Raposo, W. Stoorvogel, Extracellular vesicles, exosomes, microvesicles, and friends, J. Cell Biol. 200 (2013) 373–383, http://dx.doi.org/10.1083/jcb.201211138.
[2] M.P. Zaborowski, L. Balaj, X.O. Breakefield, C.P. Lai, Extracellular vesicles: composition, biological relevance, and methods of study, Bioscience 65 (2015) 783–797, http://dx.doi.org/10.1093/biosci/biv084.
[3] A. Lo Cicero, P.D. Stahl, G. Raposo, Extracellular vesicles shuffling intercellular messages: for good or for bad, Curr. Opin. Cell Biol. 35 (2015) 69–77, http://dx.doi.org/10.1016/j.ceb.2015.04.013.
[4] A. Becker, B.K. Thakur, J.M. Weiss, H.S. Kim, H. Peinado, D. Lyden, Extracellular vesicles in cancer: cell-to-cell mediators of metastasis, Cancer Cell 30 (2016) 836–848, http://dx.doi.org/10.1016/j.ccell.2016.10.009.
[5] S.K. Gopal, D.W. Greening, A. Rai, M. Chen, R. Xu, A. Shafiq, R.A. Mathias, H.J. Zhu, R.J. Simpson, Extracellular vesicles: their role in cancer biology and epithelial-mesenchymal transition, Biochem. J. 474 (2017) 21–45, http://dx.doi.org/10.1042/BCJ20160006.
[6] M. Surman, E. Stępień, D. Hoja-Łukowicz, M. Przybyło, Deciphering the role of ectosomes in cancer development and progression: focus on the proteome, Clin. Exp. Metastasis 34 (2017) 273–289, http://dx.doi.org/10.1007/s10585-017-9844-z.
[7] V. Padler-Karavani, Aiming at the sweet side of cancer: aberrant glycosylation as possible target for personalized-medicine, Cancer Lett. 352 (2014) 102–112, http://dx.doi.org/10.1016/j.canlet.2013.10.005.
[8] S. Pinho, C.A. Reis, Glycosylation in cancer: mechanisms and clinical implications, Nat. Rev. Cancer 15 (2015) 540–555, http://dx.doi.org/10.1038/nrc3982.
[9] S.R. Stowell, T. Ju, R.D. Cummings, Protein glycosylation in cancer, Annu. Rev. Pathol. 10 (2015) 473–510, http://dx.doi.org/10.1146/annurev-pathol-012414-040438.
[10] B.S. Batista, W.S. Eng, K.T. Pilobello, K.D. Hendricks-Munoz, L.K. Mahal, Identification of a conserved glycan signature for microvesicles, J. Proteome Res. 10 (2011) 4624–4633, http://dx.doi.org/10.1021/pr200434y.
[11] Y. Liang, W.S. Eng, D.R. Colquhoun, R.R. Dinglasan, D.R. Graham, L.K. Mahal, Complex N-linked glycans serve as a determinant for exosome/microvesicle cargo recruitment, J. Biol. Chem. 289 (2014) 32526–32537, http://dx.doi.org/10.1074/jbc.M114.606269.
[12] C. Escrevente, N. Grammel, S. Kandzia, J. Zeiser, E.M. Tranfield, H.S. Conradt, J. Costa, Sialoglycoproteins and N-glycans from secreted exosomes of ovarian carcinoma cells, PLoS One 8 (2013) e78631, , http://dx.doi.org/10.1371/journal.pone.0078631.
[13] J. Gomes, P. Gomes-Alves, S.B. Carvalho, C. Peixoto, P.M. Alves, P. Altevogt, J. Costa, Extracellular vesicles from ovarian carcinoma cells display specific glycosignatures, Biomol. Ther. 5 (2015) 1741–1761, http://dx.doi.org/10.3390/biom5031741.
[14] V.M. Abrahams, S.L. Straszewski, M. Kamsteeg, B. Hanczaruk, P.E. Schwartz, T.J. Rutherford, G. Mor, Epithelial ovarian cancer cells secrete functional Fas ligand, Cancer Res. 63 (2003) 5573–5581.
[15] K. Menck, C. Scharf, A. Bleckmann, L. Dyck, U. Rost, D. Wenzel, V.M. Dhople, L. Siam, T. Pukrop, C. Binder, F. Klemm, Tumor-derived microvesicles mediate human breast cancer invasion through differentially glycosylated EMMPRIN, J. Mol. Cell Biol. 7 (2015) 143–153, http://dx.doi.org/10.1093/jmcb/mju047.
[16] M. Herlyn, G. Balaban, J. Bennicelli, D. Guerry, R. Halaban, D. Herlyn, D.E. Elder, G.G. Maul, Z. Steplewski, P.C. Nowell, W.H. Clark, H. Koprowski, Primary melanoma cells of the vertical growth phase: similarities to metastatic cells, J. Natl. Cancer Inst. 74 (1985) 283–289.
[17] I. Cornil, D. Theodorescu, S. Man, M. Herlyn, J.A. Jambrosic, R.S. Kerbel, Fibroblast cell interactions with human melanoma cells affect tumor cell growth as a function of tumor progression, Proc. Natl. Acad. Sci. U. S. A. 88 (1991) 6028–6032.
[18] I. Juhasz, S.M. Albelda, D.E. Elder, G.F. Murphy, K. Adachi, D. Herlyn, I.T. Valyi-Nagy, M. Herlyn, Growth and invasion of human melanomas in human skin grafted to immunodeficient mice, Am. J. Pathol. 143 (1993) 528–537.
[19] D. Hoja-Łukowicz, P. Link-Lenczowski, A. Carpentieri, A. Amoresano, E. Pocheć, K.A. Artemenko, J. Bergquist, A. Lityńska, L1CAM from human melanoma carries a novel type of N-glycan with Galβ1-4Galβ1- motif. Involvement of N-linked glycans in migratory and invasive behaviour of melanoma cells, Glycoconj. J. 30 (2013) 205–225.
[20] C.A. Schneider, W.S. Rasband, K.W. Eliceiri, NIH image to ImageJ: 25 years of image analysis, Nat. Methods 9 (2012) 671–675.
[21] E. Kolasińska, M. Przybyło, M. Janik, A. Lityńska, Towards understanding the role of sialylation in melanoma progression, Acta Biochim. Pol. 63 (2016) 533–541, http://dx.doi.org/10.18388/abp.2015_1221.
[22] C. Barrès, L. Blanc, P. Bette-Bobillo, S. André, R. Mamoun, H.J. Gabius, M. Vidal, Galectin-5 is bound onto the surface of rat reticulocyte exosomes and modulates vesicle uptake by macrophages, Blood 115 (2010) 696–705, http://dx.doi.org/10.1182/blood-2009-07-231449.
[23] A.S. Block, S. Saraswati, C.F. Lichti, M. Mahadevan, A.B. Diekman, Co-purification of Mac-2 binding protein with galectin-3 and association with prostasomes in human semen, Prostate 71 (2011) 711–721, http://dx.doi.org/10.1002/pros.21287.
[24] J. Kasprzyk, E. Stepień, W. Piekoszewski, Application of nano-LC-MALDI-TOF/TOF-MS for proteomic analysis of microvesicles, Clin. Biochem. 50 (2017) 241–243, http://dx.doi.org/10.1016/j.clinbiochem.2016.11.013.
[25] L. Oliveira-Ferrer, K. Legler, K. Milde-Langosch, Role of protein glycosylation in cancer metastasis, Semin. Cancer Biol. 44 (2017) 141–152, http://dx.doi.org/10.1016/j.semcancer.2017.03.002.
[26] J. Costa, Glycoconjugates from extracellular vesicles: structures, functions and emerging potential as cancer biomarkers, Biochim. Biophys. Acta 1968 (2017) 157–166, http://dx.doi.org/10.1016/j.bbcan.2017.03.007.
[27] D. Hoja-Łukowicz, M. Przybyło, M. Duda, E. Pocheć, M. Bubka, On the trail of the glycan codes stored in cancer-related cell adhesion proteins, Biochim. Biophys. Acta 1861 (2017) 3237–3257, http://dx.doi.org/10.1016/j.bbagen.2016.08.007.
[28] N. Taniguchi, Y. Kizuka, Glycans and cancer: role of N-glycans in cancer biomarker, progression and metastasis, and therapeutics, Adv. Cancer Res. 126 (2015) 11–51, http://dx.doi.org/10.1016/bs.acr.2014.11.001.
[29] M.E. Janik, A. Lityńska, M. Przybyło, Studies on primary uveal and cutaneous melanoma cell interaction with vitronectin, Cell Biol. Int. 38 (2014) 942–952, http://dx.doi.org/10.1002/cbin.10280.
[30] E. Pocheć, M. Rydlewska, M. Przybyło, A. Lityńska, Diverse expression of *N*-acetylglucosaminyltransferase V and complex-type β1,6-branched N-glycans in uveal and cutaneous melanoma cells, Acta Biochim. Pol. 62 (2015) 323–328, http://dx.doi.org/10.18388/abp.2015_1050.
[31] M. Przybyło, E. Pocheć, P. Link-Lenczowski, A. Lityńska, β1-6 branching of cell surface glycoproteins may contribute to uveal melanoma progression by up-regulating cell motility, Mol. Vis. 14 (2008) 625–636.
[32] E. Pocheć, M. Janik, D. Hoja-Łukowicz, P. Link-Lenczowski, M. Przybyło, A. Lityńska, Expression of integrins α3β1 and α5β1 and GlcNAc β1,6 glycan branching influences metastatic melanoma cell migration on fibronectin, Eur. J.

Cell Biol. 92 (2013) 355–362, http://dx.doi.org/10.1016/j.ejcb.2013.10.007.
[33] A. Hoshino, B. Costa-Silva, T.L. Shen, G. Rodrigues, A. Hashimoto, M. Tesic Mark, H. Molina, S. Kohsaka, A. Di Giannatale, S. Ceder, S. Singh, C. Williams, N. Soplop, K. Uryu, L. Pharmer, T. King, L. Bojmar, A.E. Davies, Y. Ararso, T. Zhang, H. Zhang, J. Hernandez, J.M. Weiss, V.D. Dumont-Cole, K. Kramer, L.H. Wexler, A. Narendran, G.K. Schwartz, J.H. Healey, P. Sandstrom, K.J. Labori, E.H. Kure, P.M. Grandgenett, M.A. Hollingsworth, M. de Sousa, S. Kaur, M. Jain, K. Mallya, S.K. Batra, W.R. Jarnagin, M.S. Brady, O. Fodstad, V. Muller, K. Pantel, A.J. Minn, M.J. Bissell, B.A. Garcia, Y. Kang, V.K. Rajasekhar, C.M. Ghajar, I. Matei, H. Peinado, J. Bromberg, D. Lyden, Tumour exosome integrins determine organotropic metastasis, Nature 527 (2015) 329–335, http://dx.doi.org/10.1038/nature15756.
[34] M. Przybyło, M.E. Janik, D. Hoja-Łukowicz, Bitter sweetness of malignant melanoma: deciphering the role of cell surface glycosylation in tumour progression and metastasis, in: M. Blumenberg (Ed.), Human Skin Cancer, Potential Biomarkers and Therapeutic Targets, InTech, Rijeka, 2016, pp. 63–87.
[35] S.L. Bellis, Variant glycosylation: an underappreciated regulatory mechanism for β1 integrins, Biochim. Biophys. Acta Biomembr. 1663 (2004) 52–60.
[36] J. Gu, N. Taniguchi, Regulation of integrin functions by N-glycans, Glycoconj. J. 21 (2004) 9–15.
[37] S. Yu, J. Fan, L. Liu, L. Zhang, S. Wang, J. Zhang, Caveolin-1 up-regulates integrin α2,6-sialylation to promote integrin α5β1-dependent hepatocarcinoma cell adhesion, FEBS Lett. 587 (2013) 782–787, http://dx.doi.org/10.1016/j.febslet.2013.02.002.